Macromolecules

Volume 31, Number 9 May 5, 1998

Statistical Analysis and Simulation of Pentad Distributions of Stereoblock Polypropylenes

Michael D. Bruce and Robert M. Waymouth*

Stanford University, Stanford, California 94305-5080

Received June 26, 1997; Revised Manuscript Received March 2, 1998

ABSTRACT: A method for simulating the microstructure of atactic−isotactic stereoblock polypropylene is presented. This method uses a computer program to generate stereosequences based on alternating blocks of isotactic and atactic stereosequences. Trends in observable stereochemical pentad distributions are examined, revealing that the pentad distributions become invariant above block lengths of 50 monomer units. These simulations reveal that two polymers with identical observable isotactic pentad distributions may have very different microstructures and thus different physical properties. The spectrum of an actual polymer is compared to the simulations, and it is revealed that many possible block lengths give reasonable fits but that similar values for weight fractions are obtained for each fit.

Introduction

The microstructure of polypropylene is a critical determinant of the polymer physical properties.[1] Polymer microstructure can also reveal considerable information about the polymerization mechanism.[2,3] For these reasons, the microstructure of polypropylene has been studied intensively to correlate catalyst structure, polymerization mechanism, and polymer physical properties.

The microstructure of polyolefins is conveniently examined by ^{13}C NMR.[4−6] At 100 MHz, the region of the spectrum corresponding to the pendant methyl carbon atoms displays nine slightly overlapping resonances that correspond to pentad configurational stereosequences.[7] This pentad distribution provides information about the stereosequence distribution in the polymer. Crystalline, isotactic polypropylene exhibits a large resonance corresponding to the [*mmmm*], which is the fraction of isotactic pentad stereosequences (often reported as a percentage), while amorphous, atactic polypropylene yields a statistically random distribution of all possible pentads (Figure 1).

The stereosequence distribution of polypropylene at the pentad level revealed by ^{13}C NMR can be correlated to statistical models corresponding to different polymerization mechanisms,[5,8−11] thus revealing important information not only about structure but also about the likely mechanisms of polymerization.[2] By examining the presence of peaks corresponding to stereoerrors in isotactic polypropylene, it is possible to determine whether the origin of stereospecificity is a consequence of catalyst configuration or configurations of the growing polymer chain.[12]

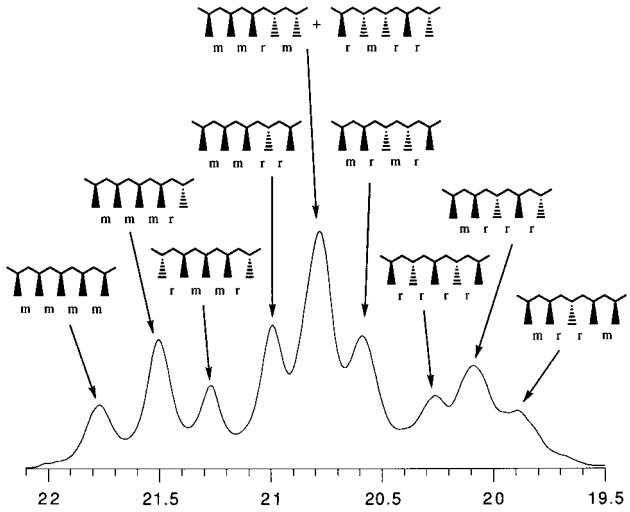

Figure 1. ^{13}C NMR and assignments for polypropylene.

We have recently reported a novel strategy for the synthesis of an elastomeric form of polypropylene using metallocene catalysts derived from nonrigid bis(2-arylindenyl)zirconocenes (Figure 2).[13−18] The elastomeric properties of this material have been interpreted in

S0024-9297(97)00942-X CCC: $15.00
Published on Web 04/17/1998

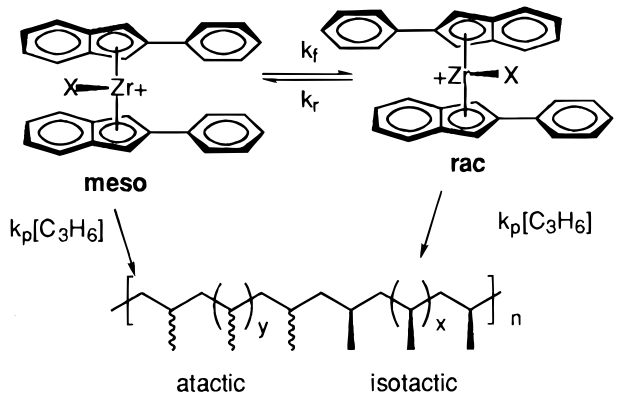

Figure 2. Proposed mechanism for synthesis of elastomeric polypropylene.

terms of a stereoblock microstructure consisting of consecutive blocks of isotactic and atactic stereosequences.[1,19−26] The stereoblock microstructure was proposed to result from an interconversion of the catalyst between chiral isospecific and achiral aspecific rotameric forms during the course of the polymerization. By varying the nature of the catalyst[14] and the polymerization conditions, these catalysts are able to produce a range of polypropylenes with different microstructures and physical properties.[13,15] A detailed understanding of the microstructure is critical to interpreting the properties of these polymers. For example, the length and distribution of the isotactic and atactic blocks are likely to be critical determinants of the elastomeric properties of these polymers. In addition, a knowledge of how the microstructure changes with changes in catalyst and polymerization conditions is critical to understanding the mechanism of polymerization with these dynamic catalysts.

Several attempts have been made to apply existing statistical models to the interpretation of the microstructure of stereoblock polypropylenes.[3,8,25,27−30] Initial models made use of analytical equations based on linear combinations of single-site mechanisms of stereocontrol (site control and chain end control). These models ignored the interfacial regions between blocks and thus were valid only for long block lengths.[3,8,27] Later models incorporate these interfacial regions via analytical equations and matrix methods.[25,29,30]

These approaches have yielded useful information, but as pointed out by Collins,[25] it is often not possible to unambiguously establish the structure and/or polymerization mechanism by modeling the pentad distribution. Part of the difficulty derives from the uncertainty in the range of possible structures that yield acceptable statistical fits to the experimentally determined pentad distribution. These limitations can be partially overcome by measuring the NMR spectra at higher field strengths that yield stereosequence distributions at the nonad level.[29,30]

In this paper, we report an approach for the analysis of stereoblock polypropylenes based on the simulation of a series of propylene microstructures using modern computational techniques. Simulations were performed to generate a library of stereoblock polymers and a corresponding library of calculated pentad distributions for each simulated chain. These studies provide an indication of the influence of various structural parameters (block length, stereospecificity within each block) on the resultant NMR spectra and how those changes correlate to the mechanism of polymerization. The simulations provide a means of ascertaining the range of polymer structures that are consistent with a given experimentally derived NMR spectrum and indicate some of the limitations of the experimental data (pentad distribution) in interpreting the microstructure of stereoblock polypropylenes.

Results

A series of microstructures of isotactic−atactic stereoblock copolymers were simulated by computer. In contrast to modeling schemes that employ probability parameters to predict stereosequence distributions,[2,3,10,11,25,27−29] the simulations generate stereosequences based on a series of fixed atactic and isotactic block lengths. These sequences may then be used both as a basis for computing pentad distributions that would be observed in a ^{13}C NMR spectrum of a polypropylene of this microstructure and to predict the length of crystallizable isotactic segments, which determine polymer physical properties.

The simulations generate model stereosequences based on four independent parameters. The first two are the atactic block length BL_a and the isotactic block length BL_i. From these two parameters, an additional useful parameter K is defined as the ratio of BL_i to BL_a:

$$K = BL_i/BL_a \tag{1}$$

The second two parameters are based on the number of stereoerrors in each block. These parameters are based on modeling schemes which have been described previously.[3−5,10] The isotactic block is assumed to have been produced under enantiomorphic site control, and thus errors are governed by the enantioface selectivity parameter α, which is the probability of a D- or L-disposed catalyst yielding a D or L stereocenter, respectively.[3] We have modeled the atactic block under both chain end control and site control, employing either the Bernoullian probability of generating a meso dyad P_m or the enantioface selectivity parameter α. Thus, each simulation is generated from four parameters: BL_a, K, α, and P_m or BL_a, K, α_1, and α_2.

A simulation consists of generating a series of stereocenters alternately producing blocks under atactic and isotactic regimes. Within a given block, each stereocenter is produced with the use of a random number generator. The random number is compared to the value of P_m or α for the particular regime and simulation to determine the stereochemistry of that center.

The number of stereocenters in a given block is determined by the block length. The block length is calculated in two ways. In the first method, the number of stereocenters in a block is equal to the block length and is determined by BL_a or BL_i, depending on the regime. Before each stereocenter is created, the modeling program determines whether the number of stereocenters created since the last change in regime is equal to the block length of the current block. If this is the case, the regime is changed to begin a new block.

In the second method, the block length is treated as the center of a Gaussian distribution; the actual block length may be shorter or longer than the input block length, but a histogram of a large sample of block lengths centers around the input block length. Here, before a stereocenter is generated, a random number is

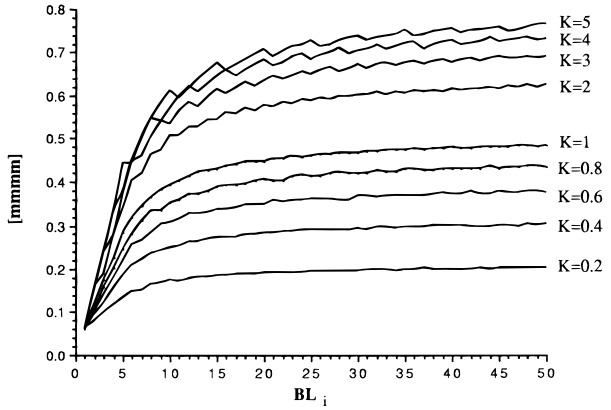

Figure 3. Effect of BL_i on [*mmmm*] for selected *K*, $P_m = 0.5$, and $\alpha = 0.99$.

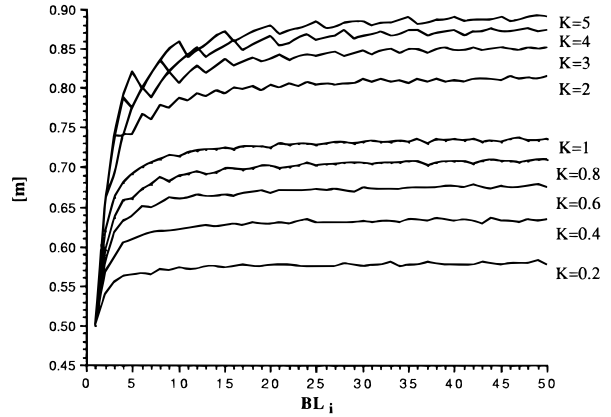

Figure 4. Effect of BL_i on [*m*] for selected *K*, $P_m = 0.5$, and $\alpha = 0.99$.

compared to a probability for switching regimes. This probability is based on the number of stereocenters created since the last change in regime and is calculated from an incomplete γ function centered on the block length. If the random number is less than the calculated probability for switching, the regime is changed.

In each method, the regime is alternated between an atactic regime and an isotactic regime. In site-controlled models, polymer is produced according to the absolute stereoconfiguration of the catalyst, which may be *R* or *S* for an isospecific catalyst. In switching regimes from atactic to isotactic, the *R* or *S* isotactic regime is selected randomly.

The simulation program was used to predict trends in polymer pentad distribution depending on trends in changing the input parameters BL_a, *K*, α, and P_m or BL_a, *K*, α_1, and α_2. Each simulation consisted of 100 000 stereocenters, approximately equivalent to the number of stereocenters in 10−50 polymer chains with M_w = 100 000−400 000. The pentad distribution that would be observed by ^{13}C NMR was counted and stored to a database, along with the parameters used to generate that simulation.

The results of the simulations reveal that the values of [*mmmm*] and [*m*] are sensitive to the length of the atactic and isotactic blocks BL_a and BL_i. For several constant values of *K* (= BL_i/BL_a), the isotactic block length BL_i was varied with $P_m = 0.5$ and $\alpha = 0.99$ (Figures 3 and 4). For a constant *K*, BL_i and BL_a increase together as defined in eq 1, and therefore an increase in BL_i for these plots represents an increase in both BL_i and BL_a. As BL_i increases, [*mmmm*] increases quickly (for $BL_i < 25$) but approaches a limiting value that depends on *K*. For $K = 0.5$, the limiting value of [*mmmm*] is approximately 0.30, while, for $K = 5$, the limit of [*mmmm*] is nearly 0.80.

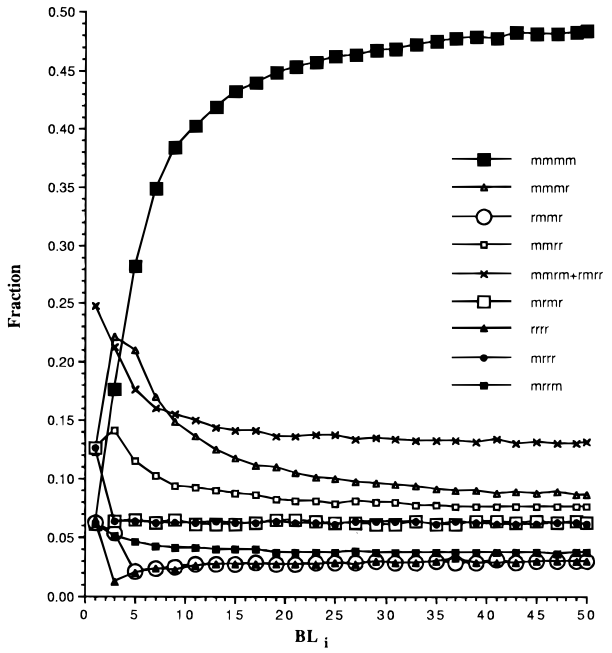

Figure 5. Effect of BL_i on all observable pentads, $K = 1$, $P_m = 0.5$, and $\alpha = 0.99$.

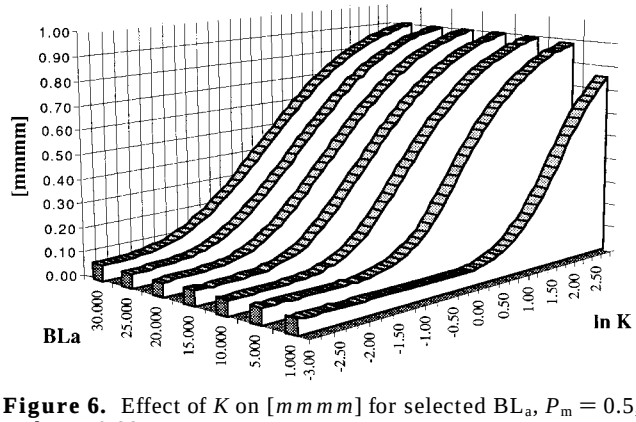

Figure 6. Effect of *K* on [*mmmm*] for selected BL_a, $P_m = 0.5$, and $\alpha = 0.99$.

An increase in the isotactic block length BL_i also results in an increase in [*m*], though [*m*] reaches saturation much more quickly ($BL_i < 10$) than [*mmmm*]. For $K = 0.5$, [*m*] saturates at [*m*] = 0.65, and at $K = 5$, [*m*] saturates at 0.90. Further analysis revealed that each of the nine observable pentads reached limiting values at $25 < BL_i < 50$ (Figure 5).

The mole fraction of isotactic pentads and dyads is very sensitive to the ratio of the isotactic and atactic block lengths $K = BL_i/BL_a$. For several constant BL_a values, *K* was varied logarithmically with $P_m = 0.5$ and $\alpha = 0.99$ (Figure 6). BL_a and *K* are related by eq 1, and therefore these plots are equivalent to changing BL_i while holding BL_a constant. For a given BL_a, atactic polymer ([*mmmm*] = 6%) is produced for values of $K < 0.1$ ($\ln K < -2$) while [*mmmm*] increases with *K* as $K > 0.1$. At very high values of BL_a, the curves converge to maximum values of [*mmmm*] for a given *K*. Similar trends were observed for [*m*] (not shown).

Changing the calculation of block length from a fixed block length to a Gaussian distribution does not change

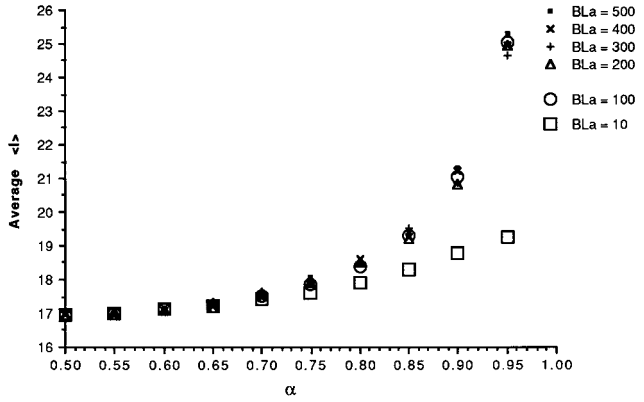

Figure 7. $[I]_{ave}$ as a function of α at $P_m = 0.5$ and $K = 1$.

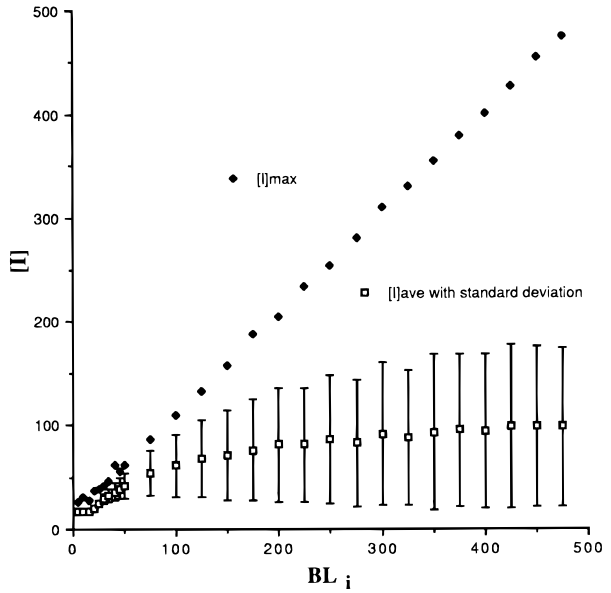

Figure 8. $[I]_{ave}$ with standard deviation as a function of BL_i.

the predicted values [*mmmm*] and [*m*]. For the same set of input parameters, the same pentad distributions are calculated for both methods of block length determination. Both fixed and Gaussian-distributed simulations reach asymptotic values at very long block lengths. For example, these asymptotic values are nearly identical for every observable pentad at $K = 1$.

An additional important structural parameter in polypropylenes is the length of uninterrupted isotactic stereosequences [*I*]. Isotactic stereosequences over 16 units in length may form crystallites.[19,31] Predicting trends in [*I*][32] should be important in predicting trends in the crystallinity of stereoblock copolymers, which in turn should be important in predicting the physical properties of the polymer. The simulations revealed interesting trends in the isotactic dyad run length [*I*] as a function of the block lengths and stereospecificities in the isotactic and atactic sequences.

As any stereoerror terminates an isotactic sequence [*I*], there are a large number of [*I*] sequences and [*I*] must be represented in several ways. The average value of [*I*], where [*I*] > 16, is represented by $[I]_{ave}$. The standard deviation of this average, $[I]_\eta$ was also calculated for each simulation. The maximum value of [*I*], $[I]_{max}$, for a given simulation is the longest stereoregular sequence for a given simulation, and N_I represents the number of uninterrupted sequences for [*I*] > 16 units in a given simulation (100 000 stereocenters). Note that

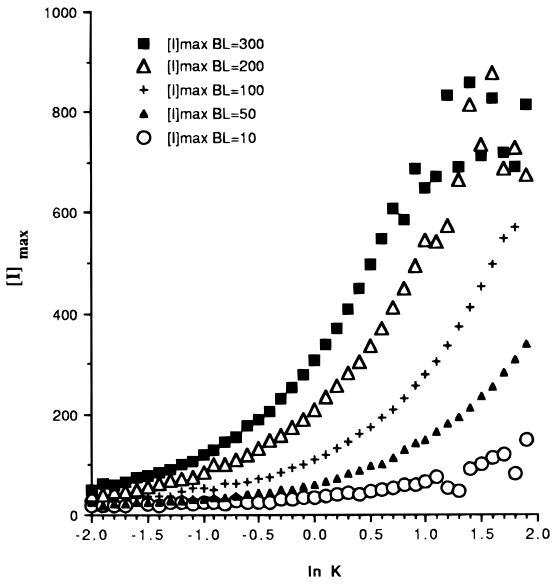

Figure 9. $[I]_{max}$ as a function of ln *K* for several BL_a values at $P_m = 0.5$ and $\alpha = 0.99$.

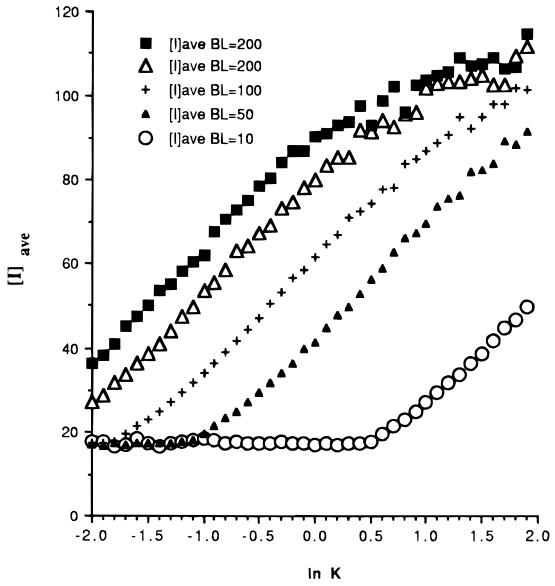

Figure 10. $[I]_{ave}$ as a function of ln *K* for several BL_a values at $P_m = 0.5$ and $\alpha = 0.99$.

$[I]_{ave}$ and N_I include only those theoretically crystallizable sequences of greater than 16 units of the same stereochemistry.

For two simulations with the same input parameters, any of these calculated values will differ because [*I*] is determined in part by a random number generator. To address repeatability, 100 repetitions of several simulations with several different inputs were performed. Each of these calculated values of [*I*], $[I]_{ave}$, $[I]_\eta$, $[I]_{max}$, and N_I varied by ±5%.

As shown in Figure 7, as α is varied for several BL_a at $K = 1$ and $P_m = 0.5$, $[I]_{ave}$ increases with increasing α. When $\alpha = 0.5$ at any BL_a, $[I]_{ave} = 17$, where [*I*] > 16. As α increased to 0.95, $[I]_{ave}$ increased to 19.5 for $BL_a = 10$ and 25.5 for $BL_a = 500$.

A series of simulations was carried out varying the block lengths BL. Each of these simulations is an average of 10 simulations of 5000 stereocenters (polypropylene $M_w = 200\,000$). As $BL_i = BL_a$ is increased from 5 to 300 ($K = 1$, $\alpha = 0.99$, $P_m = 0.5$), $[I]_{max}$ increased

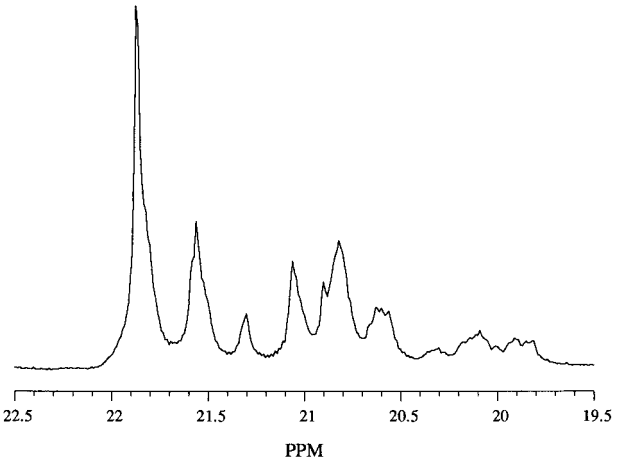

Figure 11. Quantitative ^{13}C NMR spectrum of polypropylene **2**.

steadily from 17 to 260, and N_I initially increased from 4 to 120 up to $BL_i = BL_a = 15$ and then decreased to $N_I = 20$ at $BL_i = BL_a = 300$ (Figure 11). The dependence of $[I]_{ave}$, $[I]_\eta$, and $[I]_{max}$ on changes in BL is shown in Figure 8. As $BL_i = BL_a$ increases from 1 to 500 ($K = 1$, $\alpha = 0.99$, $P_m = 0.5$), $[I]_{ave}$ increases from 17 to 100, increasing more slowly at larger BL. Additionally, the standard deviation of all $[I] > 16$ increases from 1.8 to 76.3 in this region and $[I]_{max}$ increased steadily from 27 to nearly 500.

The ratio K also influences $[I]$. When K is varied to favor the isospecific site at $BL_a = 100$, $\alpha = 0.99$, and $P_m = 0.5$, $[I]_{ave}$ and $[I]_{max}$ increase steadily (Figures 9 and 10). At $BL_a = 10$, both $[I]_{ave}$ and $[I]_{max}$ remain constant for $-2 < K < 0$, after which both increase as $K > 0$. For higher values of BL_a, there is a steady increase in both $[I]_{ave}$ and $[I]_{max}$ as K increases.

Comparison of Simulations to Experimental Spectra. The simulations described above provide a library of polymer chains whose pentad distributions have been calculated. This library can be searched for matches with experimental spectra to try to establish how many different chains (or microstructures) are consistent with a given NMR spectrum. The library of spectra was searched for matches with a sample of an elastomeric polypropylene **2** produced with bis(2-phenylindenyl)zirconium complex **1**[13] and methaluminoxane cocatalyst (1000:1 Al:Zr) in toluene solution at 75 psig propylene and 20 °C for 60 min. The resulting polymer is elastomeric and has an isotactic pentad content $[mmmm] = 26.8\%$. The ^{13}C NMR spectrum is shown in Figure 11.

The ^{13}C NMR spectrum of polymer **2** was compared to two sets of fixed block length simulations over a range of input variables (Table 1). The simulations differed in the model of propagation of the atactic block. Each simulation set was searched for a fit with **2**. The 10 best fits for each simulation are listed in Table 2.

In each case, the best fit for the simulations yields values where the stereospecificity of the atactic regions is close to random (P_m, $\alpha_1 \approx 0.5$) while those for the isotactic regions are quite high ($\alpha \approx 0.95$). The values of K are less than unity in every case, with values that range from 0.4 to 0.6 depending on the simulation set. The values of BL_a are the most scattered, with values that range from 15 to 50 but appear to cluster around 40. The best fits were obtained for simulation set 1, which was the enantiomorphic site/Bernoullian model.

Table 1. Simulation Sets and Parameters for the NMR Library

	simulation set 1	simulation set 2
BL_a[a]	1−50	1−50
K[b]	0.1−10	0.1−10
atactic parameter[c]	$P_m = 0.35-0.65$	$\alpha_1 = 0.50-0.65$
isotactic parameter[c]	$\alpha = 0.80-1.00$	$\alpha_2 = 0.80-1.00$
block length type	fixed	fixed
number of simulations in library	6×10^5	3×10^5

[a] BL_a was varied from 1 to 50 with a step size of 1. [b] K was varied from 0.1 to 1.0 with a step size of 0.1 and from 1.0 to 10 with a step size of 1. [c] Statistical effectiveness parameters were varied with a step size of 0.01.

Discussion

Various statistical models have been used to analyze the structure of polypropylene and to correlate those structures with mechanisms of polymerization.[2,5,8,10,11,25,28−30,33] The statistical parameters are based on the probability of producing a given stereocenter and depend on the type of mechanism under consideration. Polymer stereosequences which conform to Bernoullian or Markovian statistics are taken to be consistent with a single-site catalyst where stereodifferentiation is determined by stereocenters in the polymer chain (chain end control).[5] These statistical models employ conditional probabilities where subsequent stereoconfigurations depend on previous configurations. In contrast, polymer stereosequences where stereodifferntiation is assumed to be a consequence of the catalyst site, such as the enantiomorphic site model, make use of probabilities where polymer stereoconfigurations depend on catalyst configurations.[9] Concurrent models assume multiple sites and employ a weighted averages of single-site models to fit the experimental pentad distibution.

The concurrent model of Chujo[3] assumes that a blend of more than one type of polymer exists. A certain weight fraction of the polymer is produced under one model, while the remainder of the polymer is produced under another model. This concurrent model assumes that these propagating schemes occur simultaneously; each polymer chain is generated under a given model, and no interface between models is observed on any one chain. This type of model may be used to predict stereoblock microstructures for large block lengths but not for small block lengths, where the concentration of stereochemical sequences near interfaces between isotactic and atactic blocks is large. Stereosequences near interfaces can be incorporated into these statistical treatments,[8,25] but this requires additional adjustable parameters in the statistical model in order to fit the experimental spectra.

Any of these models can give information about the number and type of errors made by a given catalyst and the relative weight fractions of polymer produced by multiple-site catalysts, and have proven to be very powerful in interpreting mechanism.[2] However, these models are limited in their ability to accurately model stereoblock microstructures or to derive stereosequence distributions for block polymers. Moreover, in fitting an NMR spectrum to a statistical model, it is often difficult to ascertain the range of statistical parameters that will fit a given spectrum.[25] In particular, it is very difficult to estimate the range of isotactic block lengths that is consistent with the experimental pentad distribution.

Table 2. Best Fit Data for Simulations 1−4 with Polypropylene 2

set	RSS[a]	K	BL_a	P_m or α_1[b]	α_2	*mmmm*	*mmmr*	*rmmr*	*mmrr*	*xmrx*	*mrmr*	*rrrr*	*mrrr*	*mrrm*
exp						0.268	0.151	0.067	0.128	0.157	0.098	0.035	0.058	0.037
1	0.029 686	0.500	46	0.550	0.940	0.279	0.145	0.042	0.117	0.179	0.084	0.028	0.070	0.056
1	0.029 744	0.400	38	0.560	0.960	0.280	0.147	0.043	0.109	0.187	0.086	0.026	0.069	0.052
1	0.029 894	0.400	40	0.570	0.950	0.270	0.151	0.044	0.110	0.192	0.088	0.026	0.067	0.053
1	0.029 987	0.400	49	0.560	0.960	0.282	0.144	0.042	0.109	0.186	0.088	0.028	0.069	0.053
1	0.030 033	0.500	31	0.550	0.940	0.278	0.149	0.041	0.115	0.182	0.084	0.028	0.069	0.055
1	0.030 177	0.500	48	0.560	0.930	0.277	0.149	0.041	0.116	0.180	0.086	0.026	0.068	0.056
1	0.030 207	0.500	45	0.540	0.940	0.281	0.140	0.042	0.115	0.178	0.085	0.031	0.072	0.056
1	0.030 276	0.500	47	0.560	0.920	0.274	0.151	0.042	0.118	0.181	0.084	0.027	0.068	0.057
1	0.030 309	0.400	33	0.560	0.950	0.267	0.149	0.043	0.111	0.190	0.089	0.027	0.071	0.053
1	0.030 329	0.400	39	0.560	0.960	0.275	0.146	0.043	0.109	0.190	0.087	0.027	0.070	0.052
2	0.034 994	0.500	19	0.590	0.970	0.283	0.143	0.038	0.113	0.176	0.080	0.035	0.078	0.053
2	0.035 080	0.500	20	0.620	0.960	0.277	0.149	0.037	0.119	0.173	0.079	0.034	0.076	0.056
2	0.035 271	0.400	32	0.610	0.970	0.269	0.139	0.040	0.117	0.177	0.085	0.037	0.080	0.056
2	0.035 434	0.600	16	0.560	0.960	0.284	0.147	0.037	0.114	0.176	0.079	0.034	0.076	0.054
2	0.035 541	0.500	17	0.580	0.970	0.274	0.148	0.038	0.113	0.181	0.079	0.035	0.079	0.052
2	0.035 646	0.500	19	0.550	0.970	0.273	0.144	0.038	0.113	0.181	0.082	0.037	0.079	0.053
2	0.035 753	0.600	20	0.550	0.960	0.291	0.140	0.038	0.113	0.174	0.079	0.035	0.077	0.053
2	0.035 759	0.600	20	0.560	0.950	0.282	0.139	0.039	0.118	0.172	0.079	0.037	0.079	0.055
2	0.035 769	0.500	18	0.600	0.980	0.281	0.148	0.036	0.112	0.178	0.081	0.035	0.078	0.052
2	0.035 844	0.400	35	0.630	0.970	0.280	0.139	0.039	0.119	0.171	0.081	0.037	0.078	0.057

[a] RSS = residual sum of squares = $(\sum(I_o - I_c)^2/(I_o + I_c)$; I_o = observed intensity; I_c = calculated intensity). [b] P_m is used for simulation set 1; α_1 is used for simulation set 2.

The microstructural simulations described here create a library of microstructures of stereoblock polypropylenes. For each simulated chain, a pentad distribution is calculated and stored. This simulation technique may be used to predict how the NMR pentad distibution responds to changes in isotactic−atactic block lengths or the stereospecificity (or randomness) of the isotactic and atactic stereoblocks. In addition, by searching the library of chains for matches with experimental NMR spectra, we can get an estimate of not only the stereosequence block lengths and stereospecificity but also the range of block lengths that is consistent with a given NMR spectrum.

This simulation program was used to predict trends in pentad distribution as a function of four characteristic variables of the stereoblock polymer: the isotactic block length BL_i, the atactic block length BL_a, the degree of stereospecificity in the isotactic block α, and the degree of stereorandomness in the atactic block P_m.

As both BL_a and BL_i increase at a constant K, [*mmmm*] and [*m*] increase (Figures 3 and 4). At large BL_i, both [*mmmm*] and [*m*] approach asymptotic values that depend on K. As BL_a and BL_i approach unity, both [*mmmm*] and [*m*] collapse toward values of atactic polymers. This is likely due to the increase in concentration in interfacial regions. Since [*mmmm*] is a longer sequence than [*m*], encroachment of interfacial regions will affect [*mmmm*] at longer block lengths than [*m*]. Thus, [*mmmm*] is sensitive to BL_a for a longer span than [*m*] and saturates at higher BL.

The values of [*mmmm*] and [*m*] are quite sensitive to changes in K, the ratio BL_i/BL_a. A change in K, from $K > 0.05$ to $K < 20$ ($3.0 < \ln K < 3.0$) produces a range of $0.06 < [mmmm] < 0.90$ for an atactic block length $BL_a = 10$. Note the strong dependence of [*mmmm*] on K for $1 < K < 7.4$ ($0.0 < \ln K < 2.0$). This same value range and curve shape are seen for other values of BL_a. As BL_a increases, the curves converge to the same set of values, and K determines the asymptotic values of [*m*] and [*mmmm*]. Effectively, at large block lengths, interfacial regions become negligible and a stereoblock model converges to a concurrent model. Thus, at high BL for a given α and P_m, pentad distributions are a consequence of the weight fraction of the polymer produced at the isotactic site.

The fraction of isotactic pentads [*mmmm*] is relatively insensitive to whether the chains have fixed block lengths or a Gaussian distribution of block lengths (Table 1). This result implies that it is impossible to establish the block length distribution from experimental NMR data at pentad resolution.

Although [*mmmm*] is often used as a measure of isotacticity, the physical properties of the polymer are most strongly determined by uninterrupted runs of meso dyads which can crystallize.[32] Any stereoerror in these runs of dyads will break up the helix, lowering the degree of crystallinity.[32] To estimate the average sequence length of an isotactic stereosequence, we need to consider both the isotactic block length and the number of stereoerrors within any given isotactic block.[34] It has been proposed that an isotactic sequence of at least 11−16 units is necessary for polypropylene to crystallize.[19,31] Thus, we have calculated $[I]_{ave}$, the average isotactic sequence length, for sequences > 16 and $[I]_{max}$, the longest isotactic sequence length, for all of the simulated polymer chains.

As shown in Figure 7, an increase in the stereospecificity of the isotactic region α results in an increase in $[I]_{ave}$; likewise, $[I]_{max}$ increases steadily with increasing block lengths BL_i whereas the number of isotactic sequences > 16 drops off with increasing block length. The trends illustrated in Figure 8 show that as BL_a and BL_i increase, $[I]_{max}$ increases constantly while $[I]_{ave}$ increases and begins to level off.[35] However, the standard deviation in the average isotactic block length increases with increasing BL_a and BL_i. Thus, although the average value of [*I*] saturates, the range covered by [*I*] continues to increase with increasing lengths of the isotactic and atactic blocks BL. This is important because the longest runs of [*I*] are likely to influence the ability of the polymer to crystallize.[32]

As shown in Figures 9 and 10, the isotactic sequence lengths $[I]_{ave}$ and $[I]_{max}$ also depend on the ratio of block lengths K. For several values of a fixed atactic block length BL_a, both $[I]_{ave}$ and $[I]_{max}$ increase slowly for $K \leq 1$ ($\ln K = 0$) but increase more rapidly for $K > 1$. For values of $K < 1$, the atactic blocks are longer than the isotactic blocks; thus, there is low sensitivity of [*I*] to

changes in isotactic block length. When $K > 1$, [*I*] rises more with increasing *K*. This is consistent with the increase in isotactic block lengths that are longer than atactic block lengths at $K > 1$. This is an important result in light of the predictions of [*mmmm*]. Since [*I*] measures the actual runs of isotactic stereosequences, it is a much better predictor of polymer physical properties. Thus, analysis of the pentad distributions alone does not represent a full view of the microstructure of the polymer. This also explains why two polypropylenes of identical ^{13}C NMR pentad distributions might have markedly different physical properties. It also points to the limitation of using NMR to fully characterize stereoblock polymers.

Comparison of Simulations to Experimental Spectra. The library of simulated polymer chains and their corresponding pentad distributions can be searched and compared to experimental data. For any given experimental pentad distribution, we can identify simulated chains that would yield similar pentad distributions and thus extract the structural parameters (*K*, BL_a, α, and P_m) of simulated chains that are consistent with the experimental pentad distribution.

A sample of elastomeric polypropylene was prepared using the bis(2-phenylindenyl)zirconium dichloride/MAO catalyst, and the experimental pentad distribution (Figure 11) was compared to two different libraries of chains that were simulated using slightly different parameters. The simulations differ in that they employ two different stereospecificity parameters for the atactic blocks, a Bernoullian parameter P_m[5] or an enantiomorphic site parameter α_2.[3] A comparison of fixed and Gaussian block lengths was unnecessary, since the two methods produce identical pentad distributions.

All four simulation models produced good fits[36] with similar parameters. The best fits were in simulation set 1, which modeled the atactic blocks by Bernoullian statistics. However, these fits were very close to the fits obtained for set 2, and it is therefore impossible to ascribe either site or chain end control to the atactic block. The values of stereospecificities for the atactic blocks were all slightly greater than 0.5 but consistent with a stereorandom block. The stereospecificities for the isotactic blocks centered around 0.94, which is comparable to values observed for polymers produced from isospecific metallocene catalysts.[2,37,38]

The best matches were found for simulated chains with K ($=BL_i/BL_a$) ≈ 0.5. Searches of the database constraining $K \geq 1$ yielded several matches, but the goodness of fit values were much poorer than those with $K \approx 0.5$ (RSS ≈ 0.045). This result implies that polypropylene sample **2** has longer atactic block lengths than isotactic block lengths.

The best matches of the simulations to the experimental pentad distribution for polypropylene **2** yield values for the atactic block lengths that range from $BL_a > 17$ to $BL_a < 50$ and isotactic block lengths that range from $BL_i > 9$ to $BL_i < 25$, based on $K = 0.5$. This result again underscores the difficulty in precisely establishing the isotactic and atactic block lengths given only the pentad distributions. Despite the insufficient data provided by the pentad distribution, the simulations do provide an approximate estimate for the isotactic and atactic block lengths of polypropylene **2**.

Implications for the Mechanism of Polymerization. The simulations described above provide important structural information about stereoblock polypropylenes, but they also can yield insight on the mechanism of formation of stereoblock polypropylenes. We have reported a synthesis of stereoblock polypropylenes using metallocene catalysts derived from unbridged bis(2-arylindenyl)zirconium dichlorides.[13,14] We have proposed a mechanism (Figure 2) involving the interconversion of an isospecific chiral rac form of the catalyst and an aspecific achiral meso form of the catalyst. Restricted rotation of the indenyl ligands is postulated as the mechanism to interconvert the two forms, resulting in alternating sequences of isotactic and atactic polypropylene. To produce a stereoblock structure, the rate of interconversion should be slower than the rate of insertion at either the isospecific or aspecific site.[21,33] According to this mechanism, the catalyst exchanges unimolecularly between an isospecific site and an aspecific site according to the rate laws in eqs 2 and 3:

$$\mathrm{d[rac]}/\mathrm{d}t = k_f[\mathrm{rac}] \tag{2}$$

$$\mathrm{d[meso]}/\mathrm{d}t = k_r[\mathrm{meso}] \tag{3}$$

and

$$K_{eq} = k_f/k_r \tag{4}$$

Propagation at either site is assumed to be second order and thus follows

$$R_{p,rac} = k_{p,rac}[\mathrm{rac}][\mathrm{monomer}] \tag{5}$$

$$R_{p,meso} = k_{p,meso}[\mathrm{meso}][\mathrm{monomer}] \tag{6}$$

Insertion occurs at a given site until the catalyst changes site, producing a block of atactic or isotactic polymer. The number of units (block length) is the ratio of the rate of propagation to the rate of rotation:

$$BL_i = R_{p,rac}/(\mathrm{d[rac]}/\mathrm{d}t) = k_{p,rac}[\mathrm{monomer}]/k_r \tag{7}$$

$$BL_a = R_{p,meso}/(\mathrm{d[meso]}/\mathrm{d}t) = k_{p,meso}[\mathrm{monomer}]/k_f \tag{8}$$

Combining eqs 7 and 4 gives

$$BL_i = K_{eq} \cdot k_{p,rac}[\mathrm{monomer}]/k_f \tag{9}$$

If we assume for simplicity that the rates of polymerization at the two sites are the same, $k_{p,rac} = k_{p,meso}$, then we can express the relative block lengths in terms of the equilibrium constant between the two forms:

$$BL_i = K_{eq} \cdot BL_a \tag{10}$$

This assumption may not be true in fact, but in the case where $k_{p,rac} \neq k_{p,meso}$, K_{eq} will represent a contribution from both the ratio of [meso]/[rac] and the propagation rate constants ($k_{p,rac}/k_{p,meso}$).

This analysis allows us to correlate the kinetic parameters of our proposed mechanism with the structural inputs that we used for the simulations of the polypropylene microstructures. The previously discussed trends of the pentad distributions (Figures 2−6) as a function of the structural parameters BL_i, BL_a, *K*, α, and P_m can now be interpreted in terms of the polymerization mechanism. Thus for example, we have previously observed that [*mmmm*] increases with increasing monomer concentration for these unbridged 2-arylindene catalysts.[13,14,17,18] This could be explained

by an increase in the stereoselectivity of the aspecific site P_m, an increase in the stereoselectivity of the isospecific site α, an increase in the isotactic block length $BL_i = k_{p,rac}[\text{monomer}]/k_f$ (Figure 3), or an increase in $K = K_{eq} = k_f/k_r$ (Figure 6). The mechanism outlined in Figure 2 predicts that only the block length of the polymer should depend on monomer concentration (eq 7 and 8); thus, we have previously proposed that the increase in [*mmmm*] with monomer concentration is a consequence of increasing block lengths. However, the simulations of Figure 3 imply that [*mmmm*] should saturate with increasing block length, which has to date not been confirmed experimentally. These simulations are thus stimulating additional experiments to look for saturation behavior in the fraction of isotactic pentads [*mmmm*].

The strong dependence of [*mmmm*] on the value of *K* (Figure 6) also has interesting implications for the design of catalysts to produce stereoblock polymers. The value of [*mmmm*] is often taken as a measure of isotacticity, which is of great importance in determining the physical properties of a polymer, including modulus, elasticity, and hysteresis.[32] The control of isotacticity is therefore critical for these systems and may be accomplished in several ways: changing the stereoselectivity of the two sites P_m and α, changing the block lengths (Figures 3 and 4), or changing the ratio of isotactic to atactic block lengths *K*. The simulations suggest that changing the block length influences [*mmmm*] and [*m*] only for short block lengths and that [*mmmm*] will have an upper limit that depends on *K*. However, both the mole fraction of isotactic pentads [*mmmm*] and the average length of an uninterrupted isotactic sequence $[I]_{ave}$ are quite sensitive to the value of *K* (Figures 6 and 10); small changes in *K* can have a large influence on the microstructure of the resulting polymer. Thus, strategies of catalyst design that control the relative stability (or activity) or the isospecific and aspecific sites are likely to have a large influence on the type of polymer produced.

The analysis of polymer **2** (Table 2) also provides interesting mechanistic insights. The simulated chains that best correspond to the experimental pentad distribution all have *K* values that center around 0.5. This implies one of two possibilities: either **1** has an equilibrium constant that favors the atactic producing site or the aspecific site is more active than the isospecific site. Previous studies on bridged catalysts suggest that isospecific catalysts are more productive than aspecific catalysts.[39] If this is also true for the unbridged catalysts, the low values of *K* imply that the active catalyst derived from bis(2-phenylindenyl)zirconium dichloride exists predominantly in the achiral form during the polymerization.

Conclusions

In summary, the results of the simulations imply that the microstructure of a stereoblock polymer cannot be fully determined from the ^{13}C NMR spectrum at pentad resolution. Examination of the trends of observable pentads reveals that, for stereoblock polymers, the NMR pentad distribution is sensitive to the length of the isotactic and atactic block lengths only for block lengths < 30 monomer units. However, the average length of crystallizable isotactic sequences [*I*] is sensitive to changes in the block lengths BL and the ratio of the isotactic/atactic block lengths *K* at all values spanned by these variables. This is significant because [*I*] is likely a better determinate of polymer physical properties than [*mmmm*], and indicates that two polymers with identical ^{13}C NMR spectra might have different physical properties.[40] These simulations calculated sequences at the pentad level; recent studies have shown that sequences up to the nonad level can be assigned and measured.[28,29] While the distribution of nonads will clearly provide more information about the microstructure than pentads, we can expect a similar indeterminacy (albeit at block lengths > 30 monomer units) in establishing the isotactic and atactic block lengths, even at nonad resolution.

Catalysts derived from the unbridged metallocene **1** yield an elastomeric polymer. The properties of these polymers are proposed to derive from an atactic/isotactic stereoblock microstructure. Fitting of these simulations to a spectrum revealed a large range of possible fits, and thus absolute determination of both the polymer microstructure and the catalyst kinetic parameters was not possible. It is possible to estimate ranges of values for the microstructure of this polymer: $K \approx 0.5$, $P_m \approx 0.55$, $\alpha \approx 0.94$, and $BL_a \approx 17-40$.

Experimental Section

General Comments. Bis(2-phenylindenyl)zirconium dichloride was prepared and propylene polymerized as previously described.[13]

Polymer microstructure was determined from the methyl pentad region of the polymer ^{13}C NMR spectrum. ^{13}C NMR spectra were recorded on a Varian XL-400 spectrometer operating at 100 MHz. All polymer ^{13}C spectra were deconvoluted on a Silicon Graphics Indigo workstation using Felix.

All simulations were performed on an IBM RS-6000 computer running UNIX, using locally written routines. The random number generator and incomplete γ function were imported from *Numerical Recipes in C*.[41]

Acknowledgment. We acknowledge Amoco Chemical Company and the National Science Foundation (Grant DMR-9258324) for financial support of this work.

Supporting Information Available: Simulator.c program code for the simulation of pentad distributions of stereoblock polypropylenes (12 pages). This material is contained in many libraries on microfiche, immediately follows this article in the microfilm version of the journal, can be ordered from the ACS, and can be downloaded from the Internet; see any current masthead page for ordering information and Internet access instructions.

References and Notes

(1) Natta, G. *J. Polym. Sci.* **1959**, *34*, 531−549.
(2) Ewen, J. A. *J. Am. Chem. Soc.* **1984**, *106*, 6355−6364.
(3) Inoue, Y.; Itabashi, Y.; Chûjô, R.; Doi, Y. *Polymer* **1984**, *25*, 1640−1644.
(4) Zambelli, A.; Locatelli, P.; Provasoli, A.; Ferro, D. R. *Macromolecules* **1980**, *13*, 267−270.
(5) Bovey, F. A. *High-Resolution NMR of Macromolecules*; Academic Press: New York, 1972.
(6) Cheng, H. N. In *Modern Methods of Polymer Characterization*; Barth, H. G., Mays, J. W., Eds.; J. Wiley & Sons: New York, 1991; pp 409−493.
(7) Zhu, S.-N.; Yang, X.-Z.; Chûjô, R. *Polym. J.* **1983**, *15*, 859−868.
(8) Cheng, H. N.; Babu, G. N.; Newmark, R. A.; Chien, J. C. W. *Macromolecules* **1992**, *25*, 6980−6987.
(9) Sheldon, R. A.; Fueno, T.; Tsunetsugu, T.; Furukawa, J. *Polym. Lett.* **1965**, *3*, 23−26.
(10) Sheldon, R.; Fueno, T.; Furukawa, J. *J. Polym. Sci. A* **1969**, *7*, 763−773.
(11) Busico, V.; Cipullo, R.; Talarico, G.; Segre, A. L.; Chadwick, J. C. *Macromolecules* **1997**, *30*, 4786−4790.

(12) Frisch, H. L.; Mallows, C. L.; Heatley, F.; Bovey, F. A. *Macromolecules* **1968**, *1*, 533−537.
(13) Coates, G. W.; Waymouth, R. M. *Science* **1995**, *267*, 217−219.
(14) Hauptman, E.; Waymouth, R. M.; Ziller, J. W. *J. Am. Chem. Soc.* **1995**, *117*, 11586−11587.
(15) Waymouth, R. M.; Coates, G. W.; Hauptman, E. (Stanford University) U.S. Patent 5,594,080, 1997.
(16) Kravchenko, R.; Masood, A.; Waymouth, R. M. *Organometallics* **1997**, *16*, 3635−3639.
(17) Bruce, M. D.; Coates, G. W.; Hauptman, E.; Waymouth, R.; Ziller, J. W. *J. Am. Chem. Soc.* **1997**, *119*, 11174−11182.
(18) Maciejewski-Petoff, J. L.; Bruce, M. D.; Waymouth, R. M.; Massood, A.; Lal, T. K.; Quan, R. W.; Behrend, S. J. *Organometallics* **1997**, *16*, 5909−5916.
(19) Collette, J. W.; Tullock, C. W.; MacDonald, R. N.; Buck, W. H.; Su, A. C. L.; Harrell, J. R.; Mulhaupt, R.; Anderson, B. C. *Macromolecules* **1989**, *22*, 3851−3858.
(20) Collette, J. W.; Ovenall, D. W.; Buck, W. H.; Ferguson, R. C. *Macromolecules* **1989**, *22*, 3858−3866.
(21) Chien, J. C. W.; Llinas, G. H.; Rausch, M. D.; Lin, G. Y.; Winter, H. H.; Atwood, J. L.; Bott, S. G. *J. Am. Chem. Soc.* **1991**, *113*, 8569−70.
(22) Mallin, D. T.; Rausch, M. D.; Lin, Y. G.; Dong, S.; Chien, J. C. W. *J. Am. Chem. Soc.* **1990**, *112*, 2030−2031.
(23) Llinas, G. H.; Dong, S. H.; Mallin, D. T.; Rausch, M. D.; Lin, Y. G.; Winter, H. H.; Chien, J. C. W. *Macromolecules* **1992**, *25*, 1242−1253.
(24) Lin, Y. G.; Mallin, D. T.; Chien, J. C. W.; Winter, H. H. *Macromolecules* **1991**, *24*, 850−854.
(25) Gauthier, W. J.; Collins, S. *Macromolecules* **1995**, *28*, 3779−3786.
(26) Gauthier, W. J.; Corrigan, J. F.; Taylor, N. J.; Collins, S. *Macromolecules* **1995**, *28*, 3771−3778.
(27) Babu, G. N.; Newmark, R. A.; Cheng, H. N.; Llinas, G. H.; Chien, J. C. W. *Macromolecules* **1992**, *25*, 7400−7402.
(28) Busico, V.; Cipullo, R.; Monaco, G.; Vacatello, M.; Segre, A. L. *Macromolecules* **1997**, *30*, 6251−6263.
(29) Busico, V.; Cipullo, R.; Corradini, P.; Landriani, L.; Vacatello, M.; Segre, A. L. *Macromolecules* **1995**, *28*, 1887−92.
(30) Busico, V.; Corradini, P.; De Biasio, R.; Landriani, L.; Segre, A. L. *Macromolecules* **1994**, *27*, 4521−4.
(31) Tullock, C. W.; Tebbe, F. N.; Mulhaupt, R.; Ovenall, D. W.; Setterquist, R. A.; Ittel, S. D. *J. Polym. Sci., Part A: Polym. Chem.* **1989**, *27*, 3063−3081.
(32) Janimak, J. J.; Cheng, S. Z. D.; Giusti, P. A. *Macromolecules* **1991**, *24*, 2253−2260.
(33) Coleman, B. D.; Fox, T. G. *J. Chem. Phys.* **1963**, *38*, 1065−1075.
(34) Note that the isotactic block length BL_i is the length of a sequence which is predominantly isotactic. If the stereospecificity α is less than unity, the longest isotactic stereosequence will in general be shorter than the isotactic block length.
(35) This leveling off may be a consequence of method; the maximum values of [*I*] increase slowly, and the number of blocks decreases slowly.
(36) Model set 1 produced fits that were within 5.5% of experimentally observed distributions, while model set 2 produced fits within 6.0%. See: Collins, S.; Gauthier, W. J. *Macromolecules* **1995**, *28*, 2253−2260.
(37) Spaleck, W.; Antberg, M.; Rohrmann, J.; Winter, A.; Bachmann, B.; Kiprof, P.; Behm, J.; Herrmann, W. A. *Angew. Chem., Int. Ed. Engl.* **1992**, *31*, 1347−1350.
(38) Rieger, B.; Jany, G.; Fawzi, R.; Steimann, M. *Organometallics* **1994**, *13*, 647−653.
(39) Chien, J. C. W.; Sugimoto, R. *J. Polym. Sci., Part A: Polym. Chem.* **1991**, *29*, 459−470.
(40) Kravchenko, R.; Masood, A.; Waymouth, R. M.; Myers, C. L. *J. Am. Chem. Soc.* **1998**, *120*, 2039−2046.
(41) Press, W. H.; Teukolsky, S. A.; Vetterline, W. T.; Flannery, B. P. In *Numerical Recipes in C*, 2nd ed.; Cambridge University Press: Cambridge, U.K., 1992; pp 274−328.

MA970942X